Engineering Failure Analysis 184 (2026) 110349

Contents lists available at ScienceDirect

Engineering Failure Analysis

journal homepage: www.elsevier.com/locate/engfailanal

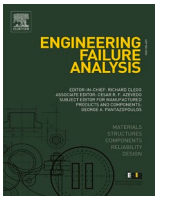

Quantification and diagnostics of Corrosion-driven energy degradation in closed loop hydronic heating systems

Amr Suliman [a,b,*], Mahroo Eftekhari [a], Vanda Dimitriou [a], Yasir Ali [a]

[a] School of Architecture Building and Civil Engineering, Loughborough University, Loughborough LE11 3UE, United Kingdom
[b] Department of Engineering Sciences, University of Oxford, Oxford OX1 3PJ, United Kingdom

ARTICLE INFO

Keywords:
Closed looped heating systems
HVAC
Water Quality
Corrosion
Filtration
Energy Performance
Experiment

ABSTRACT

Closed loop hydronic heating systems are commonly used for space heating in buildings but are prone to performance degradation due to corrosion induced fouling, an issue that remains underexplored in building services research. To this end, this novel experimental study quantifies the energy penalties associated with corrosion and evaluates the effectiveness of mechanical filtration in mitigating the corrosion effect and restoring system energy performance. A customised experimental rig was developed to simulate real world operating conditions, with corrosion mimicked by dosing 800 g of magnetite, representing up to 10–20 years of system degradation. The system was tested under various flow rates and pressures capturing different operating conditions to evaluate pump energy performance under clean, fouled, and filtered conditions. A novel non-intrusive approach using infrared thermography was used to visualise and diagnose system behaviour. Results show that corrosion induced fouling can increase pump energy consumption by up to 180 %, and in low pressure conditions, it can cause complete pump failure. Mechanical filtration restored up to 55 % of energy losses, although filter saturation led to diminishing returns, emphasising the need for maintenance. Sediment captures increased non-linearly with hydraulic loading, peaking at 460 g, but excessive accumulation risked system blockages and higher energy demand. The findings highlight the importance of water quality management to ensure optimised energy performance and operational reliability in hydronic heating systems.

1. Introduction

This research deals with the problem of improving the operational performance of closed-loop hydronic heating systems in existing buildings, aiming to enhance energy efficiency and system resilience in support of zero-carbon building objectives.

There is broad consensus within the scientific community that climate change is being accelerated by the anthropogenic release of greenhouse gases. The built environment plays a substantial role in this change, currently accounting for 39 % of global energy related emissions with 28 % arising from building operations (e.g., space conditioning and power use), and 11 % from embodied carbon associated with construction processes [1]. Notably, Heating, Ventilation, and Air Conditioning (HVAC) systems are responsible for approximately 60 % of operational energy use in buildings, underscoring the need for enhanced energy performance in this area. In response, numerous global and national targets have been established to mitigate its impact. For instance, the UK government has

* Corresponding author at: Department of Engineering Sciences, University of Oxford, Oxford OX1 3PJ, United Kingdom.
E-mail address: a.suliman2@lboro.ac.uk (A. Suliman).

https://doi.org/10.1016/j.engfailanal.2025.110349
Received 25 August 2025; Received in revised form 24 October 2025; Accepted 12 November 2025
Available online 14 November 2025

committed to achieve net zero carbon emissions by 2050 [2]. In the UK and much of Europe, hydronic heating systems are the predominant method for space heating, with radiators being employed in around 90 % of these systems [3]. Typically, such systems comprise an architecture of a central heating source, a network of pipes, and heat emitting components.

A study [4] of 259 commercial hydronic heating systems revealed that hydronic systems often operate for approximately 81 % of the year, with many functioning year-round. The study also identified that significant energy savings could be achieved through appropriate system sizing and improved water distribution temperatures. Yet, current energy saving strategies in hydronic systems tend to prioritise the generation (e.g., boilers) and dissipation (e.g., emitters) components, whilst the heat conveyance infrastructure, specifically the pipework and circulating fluid receives comparatively little attention, despite its potential for meaningful energy and cost savings [5]. Accordingly, reducing energy consumption in hydronic heating systems requires a more integrated approach, recognising the link among water quality, timely interventive maintenance, and system energy efficiency in closed loop configurations.

1.1. Corrosion in closed looped systems

Corrosion due to poor water quality is an inherent phenomenon in all hydronic systems containing metallic components. While not a new challenge, corrosion related failure and degradation have long been recognised within the built environment, with literature dating back to the early 20th century acknowledging its significance [6–9]. The severity of corrosion is highly dependent on maintenance practices and the quality of fill water, with damage reported as early as one to two years after system commissioning [10]. Although the impact of corrosion is widely studied in water distribution systems [11–17], literature specifically addressing its implications within closed-loop hydronic heating and cooling systems remains limited. A 2016 industrial study reported that up to 60 % of pipe maintenance in the oil and gas sector was attributed to corrosion [18]. A broader national assessment of corrosion costs across UK industries found that the building and construction sector accounted for over 18 % of the total national corrosion related expenditure [19]. Within building services, a survey of 53 hydronic systems evaluated based on corrosion by products and dissolved particulates revealed that 34 systems were in poor or critical condition, with one third of respondents reporting financial damage [20]. Corrosion was observed in all major system components, including pumps, pipes, valves, and heat exchangers, emphasising the pervasive nature of the problem across hydronic circuits.

A recent review on water quality and corrosion mitigation in hydronic systems highlighted that existing practices predominantly focus on the quality of filled water and its capacity to passivate dissolved oxygen within the system [21]. In the UK, The Building Services Research and Information Association (BSRIA) Guide 29 [22] supports the use of chemical inhibitors to reduce corrosion risk by passivating oxygen in the system. In contrast, the German standard VDI 2035 [23] discourages chemical inhibition, citing risks of accelerated corrosion and pitting, and advocates the use of demineralised water with low conductivity, controlled pH and minimal dissolved oxygen as a preventative strategy. Notably, these two opposing approaches have not been directly compared under controlled conditions and remain largely based on industry practice rather than empirical validation. An alternative corrosion mitigation strategy involves mechanical interventions, such as filters, dirt and air separators, and magnetic strainers [24]. Despite their widespread application, there is a clear lack of comprehensive studies evaluating their effectiveness in improving water quality, removing particulates, and restoring energy performance particularly in relation to pump efficiency and heat transfer. The most relevant available research [25] involved a controlled test on a gas boiler in a test house, assessing performance before and after the installation of an air separator. The study reported a 3.5 % reduction in boiler output required to maintain the setpoint temperature following the separator's integration. However, given that part load inefficiencies were estimated at 2.5–3 %, the actual energy saving attributable to the separator was limited to approximately 0.5 %. Another comparative study on dirt and air separators confirmed their capability to remove microbubbles of 50 μm or larger [26] but failed to address the impact of sediment removal on energy

Table 1
A Summary of findings from selected literature on corrosion in closed-loop hydronic systems, highlighting system configuration, corrosion mitigation strategy, and energy performance evaluation.

Ref	Study Type	System Type	Corrosion Mitigation Strategy	Operating Conditions Assessed?	Energy Performance Evaluated	Key Findings/Notes
20	Field Study	Closed Looped hydronic Heating & Cooling System	Water chemistry, corrosion monitoring	X	X	64 % systems in poor/critical conditions with financial damage reported.
5	Experimental	Closed Looped Hydronic Systems	Corrosion Prediction and modelling	X	X	Focus on corrosion measuring; no performance validation
25	Experimental (Test House)	Closed Looped Hydronic System (gas boiler)	Air Separator (Deaerator)	X	✔ (0.5 % Net Saving)	Slight energy reduction; confounded by part-load inefficiency and within measuring tool margin of error.
26	Experimental	Closed Looped Hydronic System	Dirt and Air Separator	✔Flow Velocity	X	Confirmed microbubble removal ≥ 50 μm; no energy data
41	Lab Test	Closed looped cooling system	Eco-friendly chemical inhibitors	X	X	Corrosion inhibitor tested; no energy metrics
43	Lab Test	Cooling Tower (Open System)	Non-chemical water treatment	X	X	Open-Loop context with limited relevance to closed loop hydronic systems

consumption or system operating conditions. Preliminary research has also suggested that flow rate influences the effectiveness of mechanical filters in capturing corrosion by products in closed loop hydronic systems [27], yet this relationship remains insufficiently quantified in the literature. An overview of the most relevant studies evaluating corrosion mitigation approaches, system types and performance impact is summarised in Table 1. From the table, key gaps in the current literature are highlighted, especially the limited assessment of energy efficiency under real-world operating conditions.

Corrosion in closed-loop hydronic systems invokes several interrelated failure mechanisms that directly affect system reliability and efficiency. These failure mechanisms include erosion-corrosion at pump impellers and other fittings under high shear [28–30], galvanic corrosion between dissimilar metals [31,32], and microbiologically influenced corrosion, in which biofilms accelerate localised pitting and under-deposit corrosion [33,34]. Furthermore, scaling due to hardness precipitation reduces heat transfer efficiency and alters flow behaviour, leading to premature failure of heat exchange surfaces [35,36], whilst magnetite deposition leads to blockages, pump seizure, and in severe cases, complete plant failure [37]. Such mechanisms drive progressive hydraulic imbalance, valve sticking, filter saturation, and heat-exchanger fouling, often culminating in premature component failure and decreased energy efficiency. The relationship between water chemistry, material selection, and operational control dictates the rate and severity of these degradation pathways, highlighting the need for integrated strategies combining chemical, mechanical, and operational interventions to enhance system longevity and performance.

Recent advancements in operational predictive maintenance technologies have introduced the use of digital twins, IoT-enabled sensing, and machine learning diagnostics for continuous health monitoring of HVAC systems [38,39]. These approaches enable real-time detection of performance anomalies, such as increased plant energy consumption (e.g., pumps), pressure fluctuations, or thermal irregularities, symptoms that can indicate fouling or blockage, integrating such data-driven tools with conventional hydronic monitoring frameworks could significantly enhance fault detection accuracy and enable proactive maintenance interventions reducing system failure and downtime. In the specific context of corrosion and water quality, continuous corrosion and system monitoring remains the most widely used method for identifying degradation and operational inefficiencies [40] However, non-intrusive, on-site diagnostic approaches are yet to be fully explored or validated for hydronic systems, presenting a promising opportunity for future exploration and adoption

1.2. Research gaps

While the role of corrosion in hydronic heating systems is widely recognised as a key contributor to operational inefficiency and premature failure, the current body of research has primarily approached the issue from material science or chemical treatment perspectives, often focusing on corrosion mechanisms and inhibitor formulations [41–44]. As summarised in Table 1, there is a clear lack of quantitative research that evaluates how corrosion-induced water quality degradation affects systems energy performance under realistic, variable operating conditions encountered in existing buildings **(research gap 1)** [45]. Additionally, although mechanical filtration is frequently implemented in practice as a corrosion impact mitigation strategy, their actual effectiveness in restoring hydraulic performance and improving energy efficiency has not been systematically validated through controlled experimentation. Previous studies have primarily concentrated on their sediment capture capabilities, without fully addressing the implications for overall system performance [25,26,46,47] **(research gap 2).** Finally, our understanding of the complex interplay between water quality parameters (e.g., particulate and corrosion content) and system operating conditions (e.g., flow rate, temperature differentials and system pressures) remains elusive and poorly addressed, limiting our understanding of its influence on hydraulic performance energy degradation in closed loop hydronic systems **(research gap 3).**

Therefore, this study aims to address these critical gaps by systematically quantifying the energy performance impact of corrosion in hydronic heating systems under a range of controlled operational scenarios. It further seeks to evaluate the effectiveness of mechanical filtration as a performance recovery strategy and to investigate how water quality and system operating parameters interact to influence hydraulic and thermal efficiency. To achieve this, a laboratory based experimental setup was developed to simulate real world hydronic conditions, allowing for detailed monitoring of thermal, hydraulic, and water content variables. Energy performance metrics are derived from empirical measurements and are analysed using non-intrusive infrared thermographic techniques to reveal parameter significance and impact on operation to support optimisation strategies.

1.3. Research novelty and contribution.

The novelty of this study lies in three primary contributions:

Firstly, the development of a controlled experimental methodology designed to isolate and quantify the energy penalties associated with corrosion-related water quality degradation under operationally relevant conditions directly **addressing Research Gap 1.**

Secondly, using the proposed experimental setup to undertake a systematic evaluation of mechanical filtration as an intervention strategy, validating its impact not just on sediment removal, but on restoring system efficiency and prolonging operational integrity, **addressing Research Gap 2.**

Finally, the application of infrared thermography as a diagnostic tool enabling real-time visualisation of thermal anomalies and flow disruptions. This non-intrusive approach supports predictive maintenance strategies and deepens understanding of the complex relationships between water quality and system operating conditions, thus directly **addressing Research Gap 3.**

The study presents two core contributions towards energy-efficient and resilient building HVAC Operation

- A validated experimental framework for quantifying the energy impact of corrosion-induced water quality degradation in closed-loop hydronic systems. The method incorporates realistic hydraulic conditions, long-term fouling simulation using magnetite, and the evaluation of performance recovery through mechanical filtration.
- The results highlight two under-recognised yet critical challenges in real-world HVAC performance. Firstly, the substantial impact of water quality deterioration and particulate fouling on component efficiency and reliability. Secondly, the essential role of continuous, non-intrusive diagnostics particularly infrared thermography to enable predictive maintenance and early fault detection. Together, these insights offer practical strategies to optimise operational efficiency and extend system longevity in support of building Net-Zero targets.

The next section details the experimental rig, including its key components and the system operating conditions used in the study. Then, the results are presented and discussed under two main outputs: (1) pump power consumption under varying corrosion and filtration states, and (2) sediment capture performance of the filtration unit. Finally, the main conclusions are outlined, with a focus on the practical implications for energy efficiency and maintenance strategies in closed loop heating systems.

2. Methods and materials

Experimental investigations of HVAC pipe networks with respect to water quality and corrosion are typically conducted using one of two approaches. The first involves passive monitoring of in-use hydronic systems through the deployment of sensors to track key parameters, such as temperature, flow rate, pressure, and water chemistry and assess their influence on overall system performance. While this method allows for continuous data collection in real operating conditions, a major limitation is the lack of control over system variables, restricting the analysis to observation alone. Additionally, in the context of corrosion, this approach is constrained by the slow nature of material degradation, which may take years to result in observable failure. The second approach focusses on experimental testing of individual components or pipe sections within a controlled environment, which is effective for comparing the corrosion performance of different materials or evaluating localised degradation mechanisms. However, it does not capture the dynamic interactions and operational behaviours of the complete HVAC system, limiting its applicability to real world performance assessments.

To investigate and quantify the impact of corrosion on a closed loop hydronic heating system, a purpose-built experimental rig was

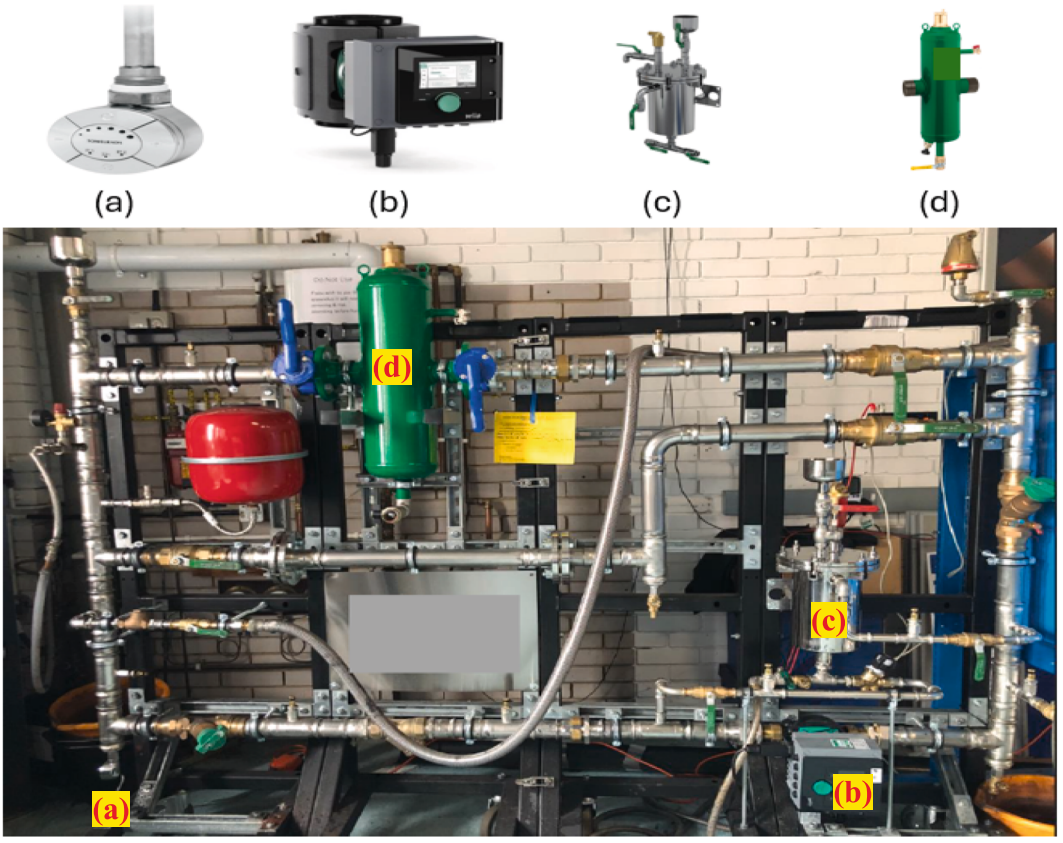

Fig. 1. A front view of the experiment rig with main components. (a) in line heater (b) pump (c) side stream filter (d) dirt and air separator.

developed. This rig allows corrosion to be deliberately introduced while enabling precise control and adjustment of system parameters for detailed analysis. Laboratory based experimental rigs are widely utilised in building services engineering research, as they provide a controlled environment to study system and component performance under reproducible conditions, including operational behaviour and fault scenarios [5,48–50]. A recognised limitation of experimental rigs is that they may not replicate the full scale or complexity of actual building systems. However, they remain valuable for simulating the physical conditions, such as temperature gradients, flow rates, and pressure levels commonly encountered in real world hydronic networks, thereby offering meaningful insight into system behaviour under controlled and accelerated conditions.

2.1. Design of the experimental rig

The setup comprises a closed loop stainless steel pipe network with a total internal volume of 18.6 Litres (Fig. 1) [51]. Stainless steel was selected to ensure the structural longevity of the rig and replicate typical material used in building services pipework. The system is equipped with a controllable heater to regulate water temperature, along with a monitoring instrumentation, including pressure gauges, flow meters, and energy meters. A detailed breakdown of the system components is summarised in Table 2. A centralised monitoring unit collects and stores all sensor data in real time, enabling continuous performance tracking. In addition, the rig includes instrumentation to monitor water quality parameters, such as corrosion rate, electrical conductivity, dissolved oxygen, and pH allowing for potential correlation between water chemistry and system performance. While these water quality measurements are integral to the system's behaviour they fall outside the immediate scope of the present study.

2.1.1. Heating plant

A 1 kW immersion heater is installed at the base of the rig to maintain and regulate water temperature throughout the experiment. The heater has a setpoint range of up to 65 °C, aligning with typical operating conditions of low temperature hot water heating systems. In this study, temperature was not treated as a variable and was therefore held constant at 55 °C for the duration of the experiments. This temperature was selected for the following reasons: Firstly, the temperature reduces risk of legionella build up in the system potentially leading to a biological contamination of the system [52]. Secondly, it represents a temperature found in low temperature heating in different building typologies.

2.1.2. Fluid circulation pump

The pump used in this study is a variable speed circulator, enabling precise control of the fluid's volumetric flow rate across predefined setpoints. This choice was made for two main reasons. Firstly, one of the aims of the investigation was to study the influence of flow rate on fouling, water quality, and energy consumption; this requires systematic adjustment of flow, which a fixed-speed pump could not provide. Second, variable-speed circulators are highly representative of modern hydronic heating systems and exhibit pronounced responses to fouling, filtration, and blockage. The selected pump is equipped with integrated sensors and onboard data logging capabilities, allowing real time measurement of key performance parameters, including flow rate, power consumption, pump

Table 2
Specifications of the main components used in the experimental rig, including the heat source, circulation pump, filtration unit, piping, and expansion vessel.

Component	Specification	Notes
Immersion heater	Type: Electric Towel Radiator Module Power Output: 1000 W Heating Range: 40 to 65 °C	Maintains constant water temperature of ≈ 55 °C during testing
Circulation Pump	Type: Variable Speed Pump Max Delivery Head: 16 *m* Max Volume Flow: 74 m^3/h Max Operating Pressure: 10 Bar Temperature Range: −10 °C – 110 °C	Provides controllable flow variation representative of closed looped hydronic systems (2 m^3/h – 6 m^3/h)
Filter Unit	Type: Side Stream Filter Max System Volume: 34,560 Litres Max Working Pressure: 4 Bar Max Flow Rate: 0.4 L/sFiltration Rate: Down to 0.5 μm (Depending on Configuration) .	Operated in bypass and active modes to assess the effects of clean, fouled, and filtered water on energy performance.
Pipes	Pipe Type: CrNiMo steel 1.4401 (EN 10088) Internal Diameter: 51 mm Surface Roughness: 1.5 μm Thermal Expansion: 0.0165 mm/(m·K)	Stainless Steel was used to ensure durability and replication of typical piping topology used in practise.
Expansion Vessel	Capacity: 8 Litres Membrane Type: Diaphragm Pre-Charge Pressure: 1.5 Bar Max Working Pressure: 6 Bar System Working Temperature Range: −10 °C – 120 °C	Provides system pressure stabilisation; with the required maximum capacity for the rig calculated as 0.28 Litres

head, and fluid temperature. These data are transmitted via a dedicated gateway to a cloud-based platform, enabling continuous remote monitoring and instantaneous data analysis. Central to this investigation is the pump's role as the primary energy consuming component within the experimental system, with its energy performance being a critical metric for assessing the effects of corrosion and fouling under varying operating conditions.

2.1.3. Mechanical filtration plant

The experimental rig was designed to accommodate two types of filtration devices: a side stream filter (Fig. 1 (c)) and a dirt and air separator (Fig. 1 (d)). For the purposes of this study, only the side stream filter was utilised. This choice was made because the dirt and air separator are installed in a series configuration, meaning it would be continuously active during system operation. As such, it would remove debris in real time, preventing the simulation of a truly fouled (dirty) system condition, thereby compromising the integrity of comparative performance assessments.

As shown in Fig. 2 (a), the side stream filter operates via a two-stage filtration mechanism. The first stage involves a magnetic strainer designed to capture ferromagnetic particles, which are typically corrosion by products. Given that a significant proportion of system debris consists of such magnetic particulates, the strainer effectively captures and retains these materials. Fig. 2 (b) presents a visual comparison of the magnetic strainer before and after sediment accumulation. The second filtration stage comprises a cartridge filter, which targets non-magnetic particulates such as sand, silt, and other fine debris that may escape the magnetic strainer. As illustrated in Fig. 2c, residual sediment not captured magnetically is effectively retained by the cartridge filter. For this experiment, a 5 μm mesh size cartridge filter was employed to ensure fine particle removal and maximise filtration effectiveness.

It is worth noting that a key methodological limitation in previous assessments [51] was that the cartridge filter was weighed without drying after sediment capture, In contrast, the methodology adopted in this study ensured that the filter was dried prior to weighing, thereby eliminating moisture variability and enabling more accurate comparison with the baseline (dry) filter mass.

2.2. System Control, Monitoring, and measurement

System monitoring and data acquisition were carried out through three primary sources: (a) a water quality monitoring unit, which was used to measure parameters such as corrosion rate, electrical conductivity, pH, pressure, temperature and flow rate; (b) a smart, data logging variable speed pump, which recorded real time values including flow rate, energy consumption, pump head, and fluid temperature; and (c) manual instrumentation comprising gauges, meters, and valves strategically placed around the rig for on-demand performance verification.

The sensor and instrumentation layout are illustrated in Fig. 3, showing the distribution of key monitoring points throughout the system. The water quality monitoring unit is equipped with multiple sensors capable of measuring both water chemistry and system

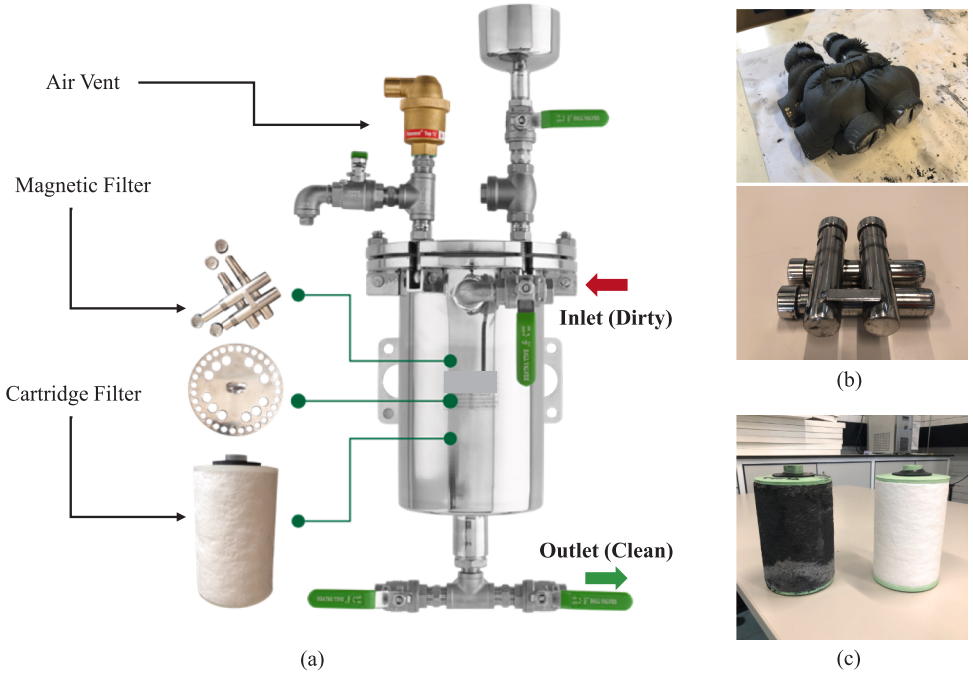

Fig. 2. (a) An illustration of the mechanical filter and its components with images of the filters before and after sediment collection for: (b) Magnetic Strainer (c) Cartridge Filter.

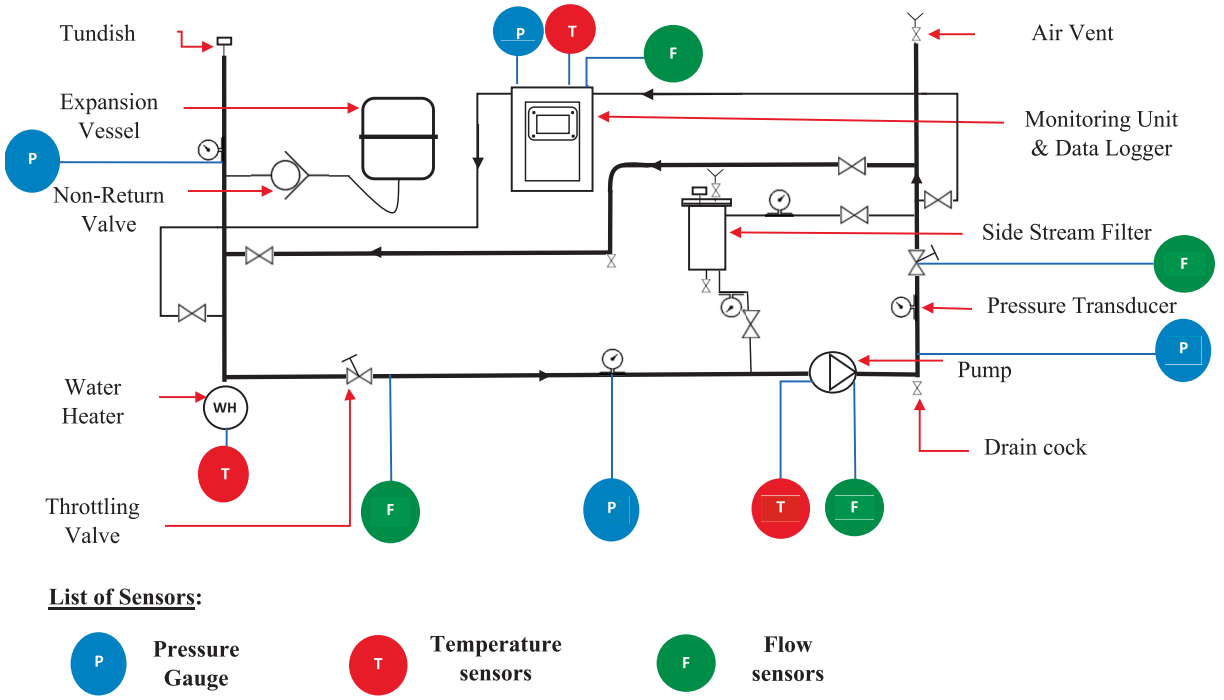

Fig. 3. A schematic diagram of the rig with the distribution of meters, gauges and sensors.

performance parameters, including pressure, temperature, and flow rate. Additionally, it monitors key water quality indicators, such as dissolved oxygen, pH, electrical conductivity, and corrosion rate factors critical to understanding and characterising corrosion processes within closed loop hydronic systems. For the purposes of this study, the unit was primarily used to monitor and log system pressure and temperature at five-minute intervals. The second primary data collection point was the variable speed pump, capturing the pumps energy performance data. Data from both the pump and the monitoring unit were combined to form a comprehensive dataset for subsequent analysis.

As shown in Fig. 3, pressure transducers were distributed throughout the rig to monitor system pressure and validate readings from the central monitoring unit. Additional transducers were positioned upstream and downstream of the filter to measure pressure differentials and confirm blockage events. Flow meters were installed for manual verification of the pump's regulated flow rate, while an external power meter at the pump's mains supply provided an independent check of energy consumption. Table 3 summarises all measurement devices, their operating ranges, and accuracies. Each key parameter was measured using at least two independent instruments, ensuring data reliability and cross-validation across all test conditions.

2.3. System operating conditions

The experimental rig was designed to replicate the characteristics of a low-pressure hot water system. According to CIBSE Guide B [53] and ASHRAE [54], LPHWS typically operates at a static pressure of 1 bar. In this study, the system was tested under three pressure conditions: 0.5 bar, representing a low-pressure scenario, 1 bar, reflecting standard design conditions, and 1.5 bar, simulating a high-pressure operating state.

Flow velocity in hydronic systems must also be carefully controlled. As detailed in CIBSE Guide B [53], high velocities in steel pipework can cause vibration and erosion corrosion, while excessively low velocities may lead to particulate deposition and the

Table 3
Summary of gauges and meters with their ranges and accuracies.

Measurement	Device	Range	Accuracy
Energy	RS Pro Energy Meter	0.0 W to 9999 W	+/- 1 %
Energy	Wilo Stratos Pump	Up to 7.5 kW	+/- 2 %
Temperature	Wilo Stratos Pump	−10° – 110 °C	+/- 0.5 K
Temperature	Hevasure Monitoring Unit	Up to 82 °C	± 0.3 °C
Flow Rate	Wilo Stratos Pump	2 – 8.2 m^3/h	+/- 5 %
Flow Rate	Venturi Valve	Up to 11.5 m^3/h	+/- 3 %
Pressure	Hevasure Monitoring Unit	Up to 10 Bar	+/- 0.5 %
Pressure	RS Pro Pressure Guage	Up to 10 Bar	+/- 2.5 %

formation of sludge, potentially requiring system flushing or mechanical intervention. For 50 mm steel pipework, the recommended maximum velocity is 1.5 m/s, while minimum recommended velocities are around 0.5 m/s to ensure effective circulation [55]. Accordingly, three flow rates were selected for testing: 2 m^3/h (0.28 m/s), representing a low flow system, 4 m^3/h (0.57 m/s), representing a design recommended flow rate, and 6 m^3/h (0.85 m/s), representing a higher than design condition. These test conditions were chosen to align with industry guidance and provide insight into how variations in system operation affect corrosion, filtration performance, and energy consumption.

2.4. Simulating corrosion in the system

Corrosion in closed loop hydronic systems is influenced by various factors, including commissioning quality, usage patterns, system age, and heat transfer fluid type. Biological factors, such as microbiological activity and scaling, can further accelerate corrosion, with oxygen ingress via depressurisation or fill water being the most critical contributor.

According to the Belgian Scientific and Technical Centre for the Construction Industry [56], systems exposed to oxygen ingress can accumulate over 4 kg of magnetite annually per 1000 L, primarily due to improperly configured variable pressure expansion vessels, while other scenarios can yield around 2 kg per 1000 L based on the causation. As such, the reference values of 2 kg and 4 kg per 1000 L per year will be used for this investigation [56]. To emulate long-term corrosion fouling, 800 g of magnetite (Fe_3O_4) was introduced to the closed loop. The equivalent operating years are calculated as per Eq. (1):

$$years = \frac{M \times 1000}{r \times V} \tag{1}$$

Where, $\boldsymbol{M}$ is the injected magnetite mass (kg), $\boldsymbol{V}$ is volume of the rig (Litre), and $\boldsymbol{r}$ is the debris build up (kg per 1000 L.year^{-1}). For $\boldsymbol{M}$ = 0.80 kg, $\boldsymbol{V}$ = 18.6 L (Measured Volume of the Rig) and $\boldsymbol{r}$ = 2–4 kg per1000 L.year^{-1} [56], the dose represents ≈10–20 years of corrosion accumulation in the system, which corresponds with the typical service life of closed-loop hydronic heating system components [57].

The dried magnetite powder was injected via the dosing tundish located at the highest point of the rig following system depressurisation. The powder was added incrementally to promote suspension and prevent local accumulation or immediate clogging, with the pump operating at low speed to aid uniform dispersion. After all magnetite had been dosed, the system was repressurised and circulated for several minutes to ensure complete mixing before testing commenced. This controlled dosing procedure ensured repeatable and homogeneous fouling conditions across all test runs.

It is recognised that corrosion and fouling rates vary widely depending on system design and operation. As outlined in BSRIA BG 50 [24], key influencing factors include materials of construction, control strategy, system volume, and the chemical and physical water treatment applied. Similarly, VDI 2035 [23] highlights the influence of fill-water chemistry, particularly pH, conductivity, and salinity on corrosion initiation and progression. Accordingly, the reference range of 2–4 kg per 1000 L·year^{-1} used to derive the 800 g magnetite loading in this study represents an indicative envelope capturing typical to severe real-world corrosion scenarios.

2.5. Infrared thermography for monitoring system performance

A FLIR T1K thermal imaging camera was employed to perform non-intrusive diagnostics and monitor the thermal behaviour of the

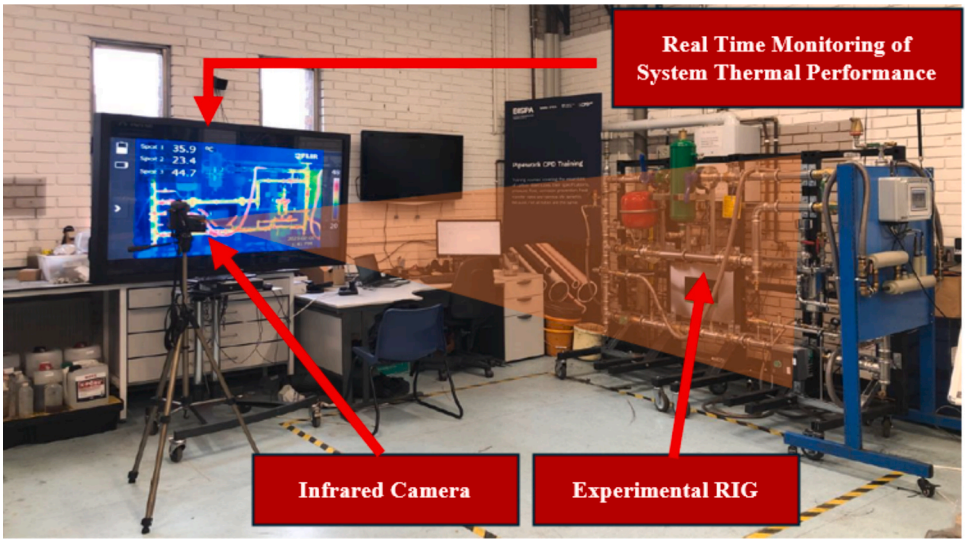

Fig. 4. Experimental setup showing infrared thermography system used for real-time thermal monitoring of the hydronic rig, including the camera, the experimental testbed, and the live thermal display.

hydronic system in real time. This approach enabled the visualisation of temperature distributions and identification of flow anomalies without disrupting system operation. Fig. 4 illustrates the setup, showing the camera positioned in front of the experimental rig and the corresponding live thermal feed displayed on a monitoring screen. The camera has an Infrared sensor resolution of 1024 x 768 (786, 432 pixels) and a temperature range of −40 °C to 2000 °C, with an accuracy of ± 1 % for temperature ranges between 50° to 150 °C.

3. Results and discussions

The sequence of testing begins with a 24-hour run under clean conditions (no corrosion) to establish baseline performance at the specified flow rate and pressure. In the second stage, 800 g of magnetite is dosed into the rig to simulate a fouled system, which also operates for 24 h. In the third stage, the filter bypass is opened, and the system is run for an additional 24 h to assess sediment removal and performance recovery. This sequence as presented in Fig. 5 is repeated for all combinations of flow rate and pressure with their results presented in this section.

3.1. Pump failure due to fouling accumulation

Fig. 6 illustrates the power consumption behaviour of the pumping system operating at a constant flow rate of 2 m3/h under two pressure settings: 1 bar and 1.5 bar. Experimental trials conducted at 0.5 bar were excluded from the performance analysis due to pump failure observed under fouled conditions. In this context, 'pump failure' refers to loss of hydraulic functionality, characterised by unstable power consumption, erratic head generation, and eventual cessation of fluid circulation. This behaviour was attributed to sediment accumulation and partial blockage at the pump suction, which impeded flow under low-pressure conditions. Fig. 7 presents the corresponding pump failure alert alongside visual evidence of fouling deposition at the pump base. At 1 bar, the average power consumption increased from 11.74 W under clean conditions to 15.70 W when the system was fouled, representing a 33.7 % rise due to increased hydraulic resistance. Upon activation of the filtration unit, the average power demand decreased to 13.53 W, corresponding to a 54.8 % recovery of the excess energy loss induced by fouling. A similar trend was observed at 1.5 bar. The clean state power demand remained consistent at 11.74 W, while fouling elevated the average consumption to 15.52 W. Filtration reduced this consumption to 13.66 W, yielding a 49.2 % mitigation of the fouling induced power penalty.

The pump failure observed at 0.5 bar under fouled conditions highlights the susceptibility of low-pressure hydronic systems to sediment accumulation, which can cause complete hydraulic breakdown. This behaviour is consistent with previous studies reporting that low flow velocity and insufficient pressure differentials promote particulate deposition and impeller blockage, leading to centrifugal pump failure [58,59]. While the activation of real-time filtration enabled partial recovery of energy efficiency at higher pressures, these findings emphasise the necessity of maintaining adequate flow and pressure to prevent sediment buildup and ensure stable, uninterrupted operation.

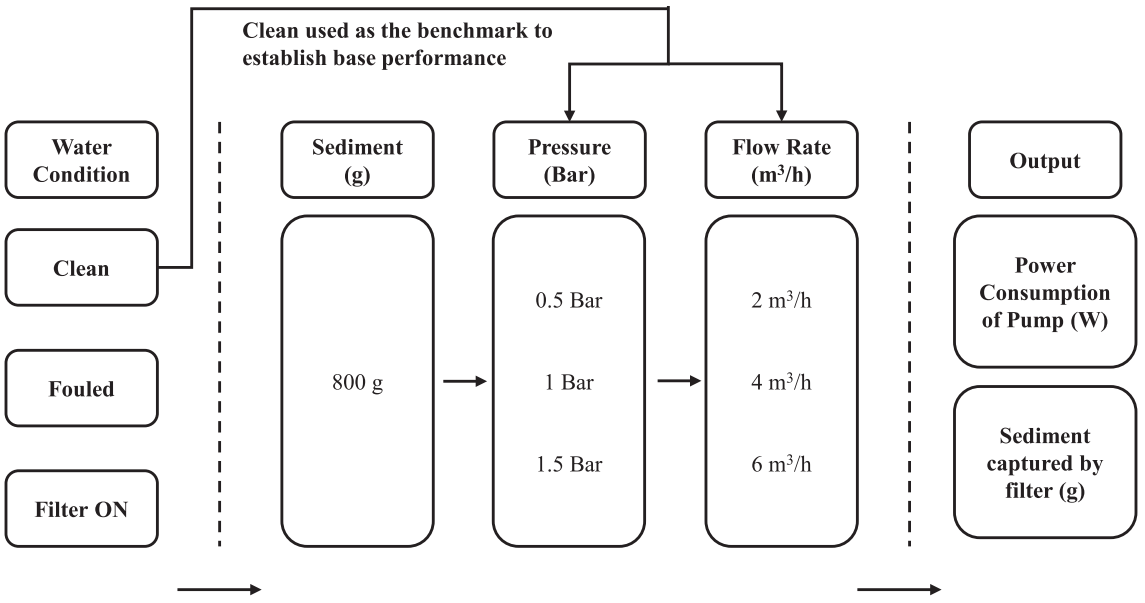

Fig. 5. Experimental matrix outlining the test conditions and data collection approach used to assess the impact of corrosion and filtration on pump energy performance in a closed loop hydronic system.

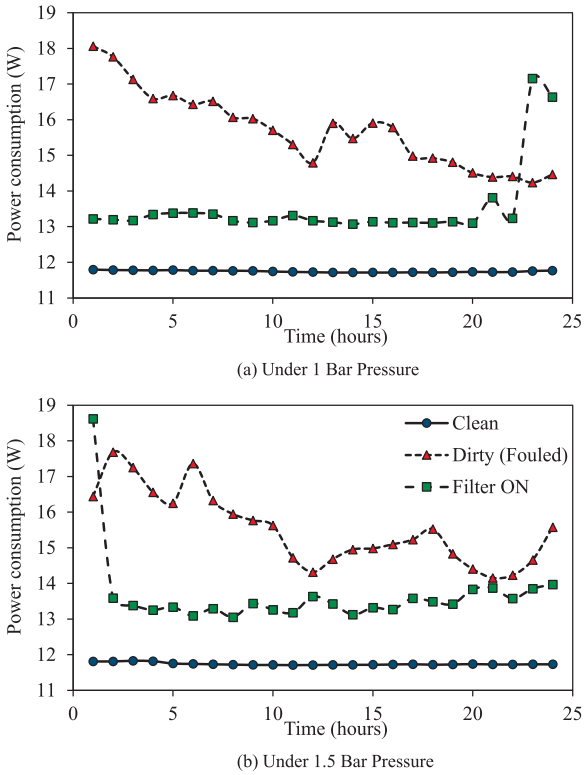

Fig. 6. Pump power consumption over 24 h at a flow rate of 2 m^3/h under two pressure conditions (1.0 and 1.5 bar), comparing three system states: Clean (fouling-free baseline), Fouled (after magnetite dosing to replicate corrosion by-products), and Filter ON (with the filtration unit activated to remove suspended sediments).

Fig. 7. (a) The pump failure message due to the fouling accumulation on the pump shaft. (b) fouling build up on the pump inlet.

3.2. Pump energy consumption due to fouling

Following an increase in flow rate to 4 m3/h, the system's response under varying pressure conditions is shown in Fig. 8. At the lowest pressure setting (0.5 bar), the introduction of magnetite fouling caused a dramatic rise in power consumption from 18.92 W under clean conditions to an average of 53.09 W, representing a 180.7 % increase. However, no pump failure was recorded as observed under the flow rate of 2 m^3/h, due to increased flow velocity limiting sedimental suspension on the pump. Activation of the filtration unit reduced power demand to 39.31 W, corresponding to a 46.4 % recovery of the fouling induced energy loss. A pronounced surge in power consumption was observed between the first and third hour under fouled conditions. Non-intrusive thermographic imaging diagnostics, depicted in Fig. 9, confirmed the presence of blockages forming within the hydraulic circuit, which coincided with the abrupt increase in pump workload.

At 1 bar, a similar trend was evident. Power consumption rose from a clean state average of 25.19 W to 39.23 W under fouled

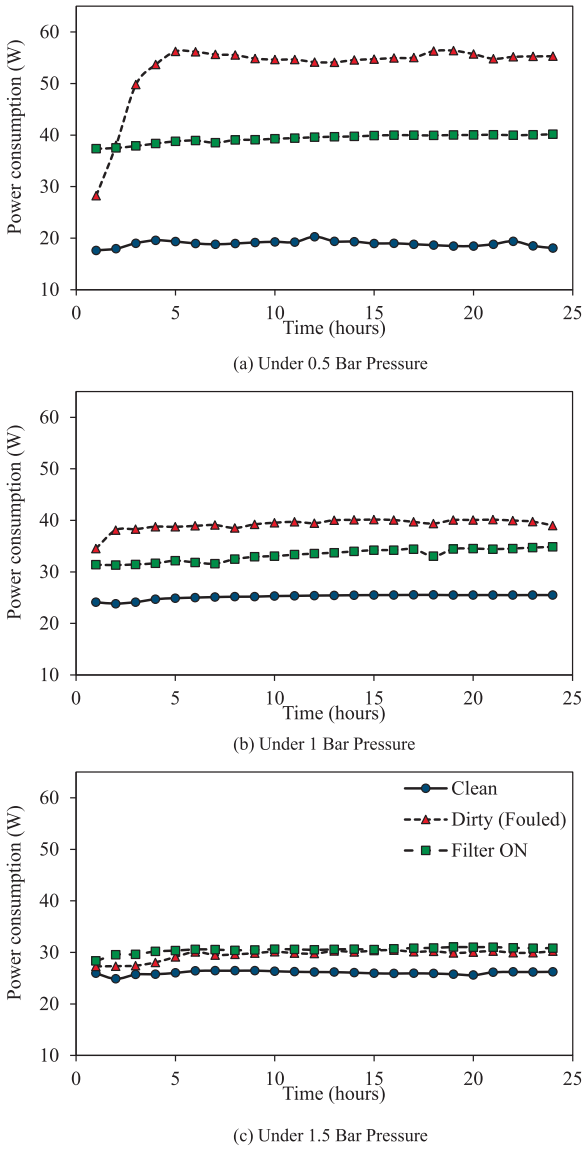

Fig. 8. Pump power consumption over 24 h at a flow rate of 4 m^3/h under three pressure conditions (0.5, 1.0 and 1.5 bar), comparing three system states: Clean (fouling-free baseline), Fouled (after magnetite dosing to replicate corrosion by-products), and Filter ON (with the filtration unit activated to remove suspended sediments).

conditions, an increase of 55.7 %. With active filtration, the average demand fell to 33.25 W, achieving a 42.4 % restoration. Conversely, at 1.5 bar, the impact of fouling was substantially lower. Power consumption increased modestly from 26.06 W (clean) to 29.57 W (fouled), a rise of just 13.5 %. The Filter ON condition averaged 30.47 W slightly exceeding the dirty state consumption. This marginal increase (3 %) may be attributed to additional system head losses or parasitic energy overhead introduced by the filtration mechanism itself. The reduced fouling sensitivity observed at 1.5 bar is consistent with reports that increased hydraulic stability and wall shear stress at higher flow intensities suppress particulate adhesion and promote resuspension, thereby limiting deposit formation under turbulent conditions [60,61]. Although static pressure alone does not directly increase wall shear, operation at higher pressures in closed-loop systems is typically accompanied by more stable flow behaviour and reduced stagnation, mitigating fouling tendencies.

3.2.1. Energy penalty relative to building scale

Although the absolute pump power measured in this study (10–80 W) appears small relative to total HVAC demand, the observed 180 % increase in energy consumption under fouled conditions has notable cumulative implications. A review of hydronic heating systems found that such systems typically operate for approximately 81 % of hours annually [4]. Assuming a 50 W variable-speed circulator, typical of a central heating application operating 81 % of the year (≈ 7,096 h), fouling increases annual energy consumption from approximately 355 kWh to 993 kWh, representing an additional 638 kWh per pump. At an emission factor of 0.20 kg

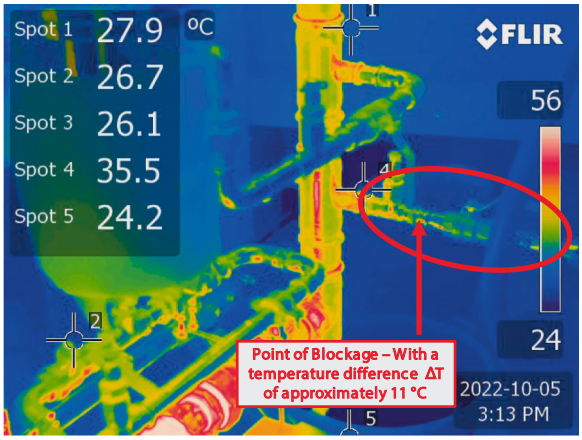

Fig. 9. An infrared thermographic image of a blockage occurrence due to fouling under the flow rate of 4 m^3/h and 0.5 Bar pressure, with a temperature difference of 11 °C observed pre and post blockage.

CO_2 kWh^{-1} [62], this corresponds to 0.13 tonnes of CO_2 per year. When scaled across multiple pumps, this additional 638 kWh yr^{-1} per pump equities to several megawatt-hours per year in multi-pump arrangements, representing a substantial sum of HVAC energy consumption. This reinforces the importance of maintaining water quality and implementing proactive fouling control measures in closed-loop hydronic systems.

3.3. Infrared thermographic diagnostics of blockages in pipes

Increasing the flow rate to 6 m^3/h starts to show a more volatile system behaviour at a pressure of 0.5 bar, fouling resulted in a significant increase to a mean value of 61.01 W, reflecting a 91.6 % increase in energy demand. From the fourth hour, the power consumption increases significantly before it stabilises around the 80 W mark. Thermographic imaging, as presented in Fig. 10 (a), reveals that fouling has caused partial to complete blockages at several locations throughout the system. These obstructions have significantly impeded fluid circulation, contributing to the observed spike in energy usage. Post operational diagnostics confirmed the presence of solidified magnetite clusters within the pipework. Visual confirmation of these blockages is provided in Fig. 10 (b) and (c), where the affected pipe runs exhibit clear evidence of restricted flow pathways due to particulate buildup.

Fig. 11 quantifies the axial pipe surface temperature profiles obtained from thermographic analysis across blockage points b (Fig. 11a) and c (Fig. 11b). In both pipe sections, when no blockage was present, the temperature difference (ΔT) along the pipe remained stable at approximately 3–4 °C, indicating uniform heat transfer and unrestricted flow. However, under blocked conditions, ΔT increased noticeably rising to 10 °C at point b and reaching up to 13 °C at point c. These elevated temperature gradients are consistent with restricted circulation and diminished convective heat transfer. Accordingly, a ΔT exceeding ≈ 10 °C can be proposed as a quantitative threshold for predicting blockage onset or severe fouling within closed-loop hydronic heating systems, providing a practical diagnostic criterion for condition-based maintenance.

In practice, pressure differential monitoring is the standard method for detecting blockages in closed-loop hydronic systems. However, this technique alone cannot accurately locate the fouling site or differentiate between filter saturation and inlet blockage. The integration of infrared thermography in the present setup addressed this limitation by visualising temperature gradients associated with restricted flow regions, thereby enabling direct identification of blockage location and severity. This diagnostic capability represents an innovative and practical approach for detecting and contextualising blockage and filter saturation-related performance degradations, providing insight into their underlying causes, a level of diagnostic resolution previously not achievable using pressure differential monitoring alone [63].

3.4. Impact of filter saturation on pump energy consumption

Under 1 bar pressure and flow rate of 6 m^3/h, the system exhibited the highest overall energy penalty associated with magnetite fouling (Fig. 12b). Average pump power increased from 37.96 W under clean conditions to 70.91 W when fouled, an 86.8 % rise. Although slightly lower than the 0.5 bar case, this condition yielded the greatest absolute power demand, indicating that 1 bar represents a transitional operating point where flow turbulence is insufficient to prevent deposition, yet pressure is high enough to sustain continuous circulation and fouling accumulation. Activation of the filter reduced mean power consumption to 46.61 W, a 34.3 % improvement relative to the fouled state.

Filter saturation was identified as a critical hydraulic failure mode where sustained operation revealed a gradual decline in filtration effectiveness. Across all pressure conditions, pump energy initially decreased after filter activation but subsequently increased with time. This fouling mechanism arises when trapped particulates accumulate on the filter mesh, restricting flow and elevating hydraulic resistance. This restriction promotes the formation of stagnant and recirculating zones that further accelerate

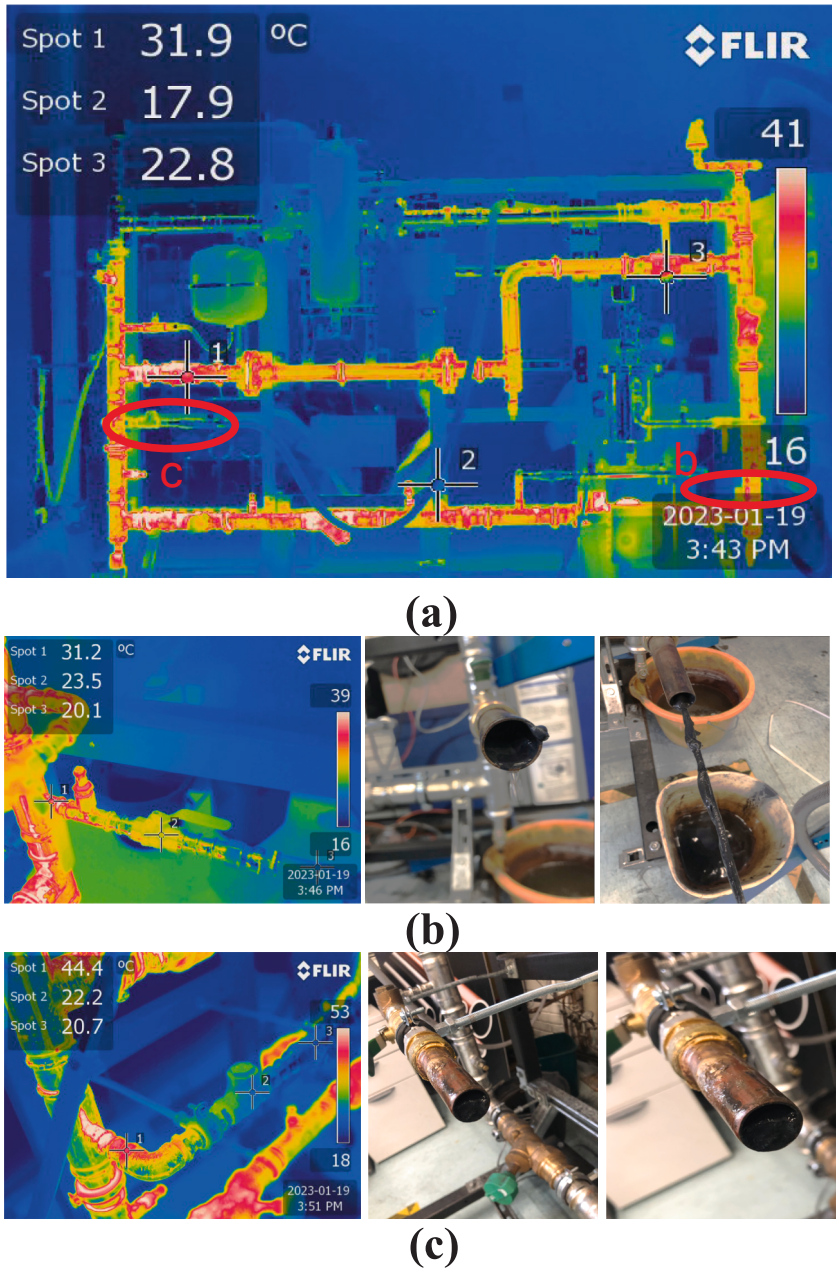

Fig. 10. Diagnosis of internal blockages using infrared thermography. (a) Thermal image of the full experimental rig (b) close-up thermograph and post intrusion photographs revealing sediment accumulation and blockage at b; (c) close-up thermograph and physical inspection at blockage location, showing corrosion induced buildup within the pipework at c.

deposition and particle build-up on the filter site. This was reported in other studies, citing velocity and flow as a key parameter influencing filter saturation [64].

Thermographic evidence in Fig. 13 supports this interpretation. During active filtration (Fig. 13a), the filter surface temperature stabilised at approximately 24 °C, identical to post-filtration conditions (Fig. 13b). The absence of measurable thermal variation across states indicates stagnant fluid and no convective heat transfer, confirming that internal blockage restricted flow through the filter housing. Comparable results were observed at 1.5 bar, further validating that filter saturation resulted in the observed loss of performance. Such performance deterioration reflects a key limitation of passive magnetic filtration systems, while initially effective, are prone to performance reversal when not periodically maintained.

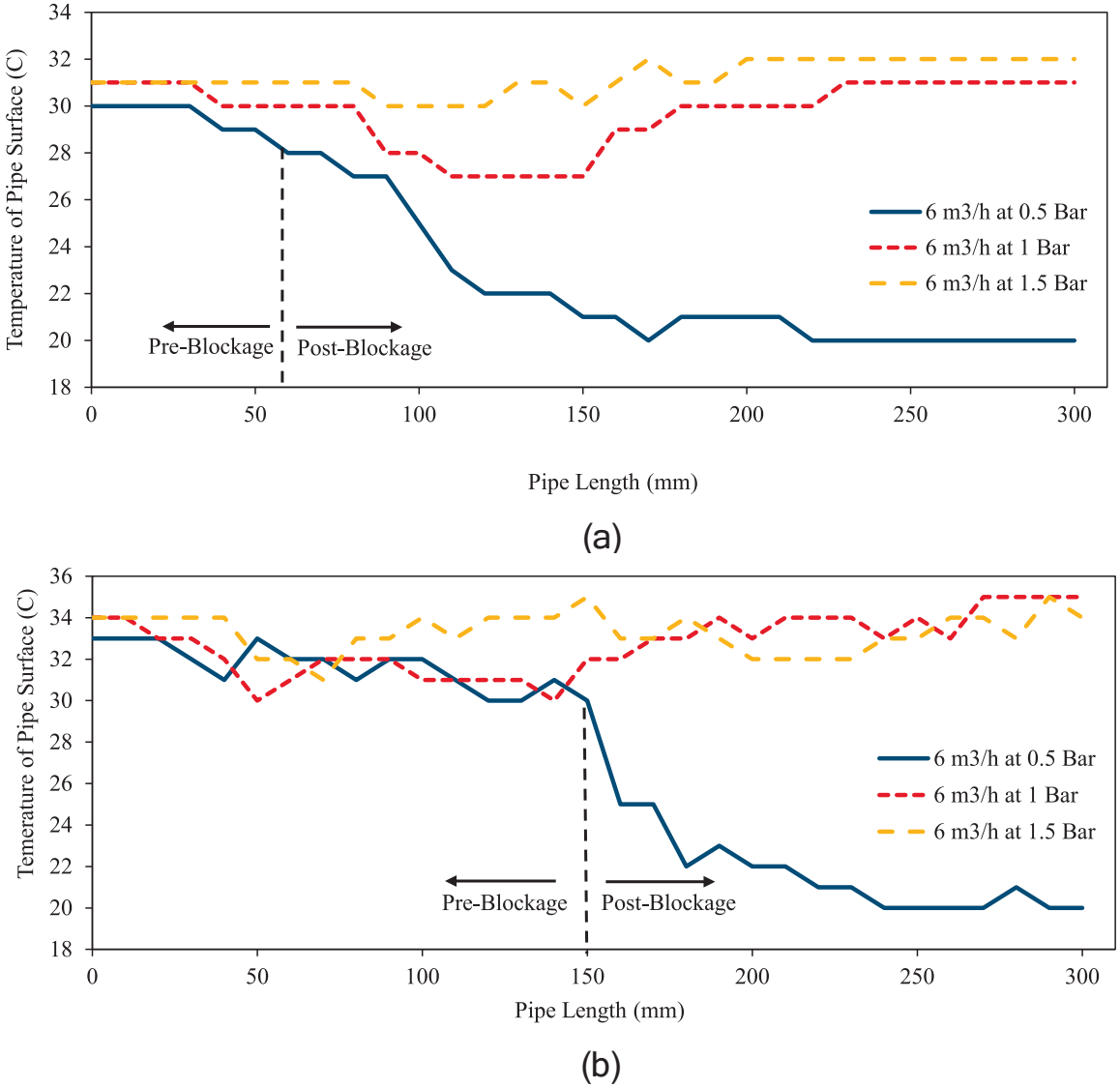

Fig. 11. Axial pipe surface temperature distributions obtained from infrared thermography at a constant flow rate of 6 m^3/h under three pressure conditions (0.5, 1.0, and 1.5 bar). (a) Temperature profile across blockage point b and (b) blockage point c.

3.5. Sediment capture by the filter

The sediment capture results reveal a clear and positive correlation between the hydraulic loading (pressure and flow rate) and the amount of sediment retained by the filter, with distinct groupings visible across the tested conditions. From Fig. 14, at a flow rate of 2 m^3/h, sediment capture remained minimal across all pressures, ranging between 0 and 19 g. These low values reflect limited particulate transportation under reduced flow velocities and shear forces conditions that are less favourable to sediment entrainment. The analysis of the 0.5 bar pressure condition revealed that under all conditions, system failure and blockage occurred before the filter was introduced, hence its low efficiency. When the flow rate increased to 4 m^3/h, sediment capture rose substantially, particularly at higher pressures. At 1 bar and 1.5 bar, the system collected 151 g and 244 g of sediment respectively, indicating enhanced transport and delivery of particulates to the filter. This improvement is likely due to increased turbulence and fluid shear stress, which promote the resuspension of settled sediments.

At a flow rate of 6 m3/h, sediment capture peaked at 460 g under 1.5 bar and 455 g under 1.0 bar operating pressure. Both conditions resulted in filter saturation, evidenced by a marked increase in system power consumption under filtering conditions (Fig. 12) and thermographic indications of stagnant flow, confirming the onset of blockage (Fig. 13). This empirically established operational limit demonstrates the existence of a practical upper threshold to the filter's sediment-holding capacity. Once this threshold is reached, the filter becomes progressively restrictive, leading to increased hydraulic resistance and a corresponding decline

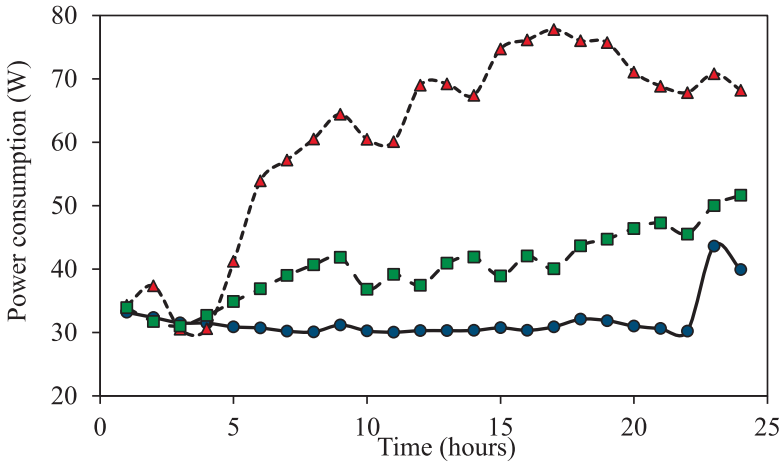

Fig. 12. Pump power consumption over 24 h at a flow rate of 6 m^3/h under three pressure conditions (0.5, 1.0 and 1.5 bar), comparing three system states: Clean (fouling-free baseline), Fouled (after magnetite dosing to replicate corrosion by-products), and Filter ON (with the filtration unit activated to remove suspended sediments).

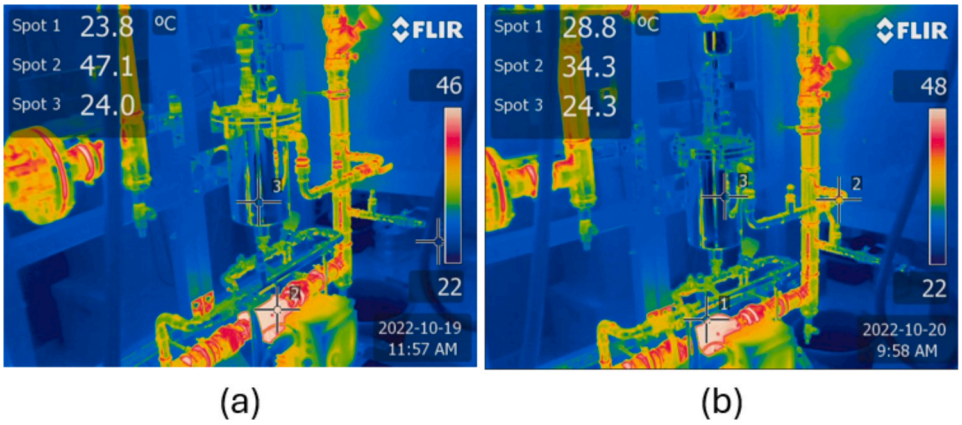

Fig. 13. A thermographic image of the filter (a) during operation and (b) after filtering (Turned OFF) highlighting a blockage during operation.

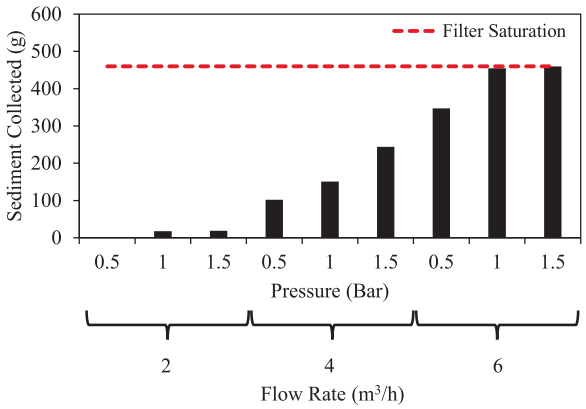

Fig. 14. Mass of Sediment collected under varying pressure and flow rate conditions, with the red dashed line indicating the saturation limit of the filter.

in energy performance.

These findings illustrate that sediment transport and filtration effectiveness increase non-linearly with both pressure and flow rate, particularly beyond critical operational thresholds. The sharp rise in sediment accumulation at higher hydraulic intensities underscores the importance of optimising system parameters. This compliments previous research in other systems which states that system parameters such as flow rate and system pressure plays a dominant role in filtration performance [64,65]. A carefully balanced approach to flow rate and pressure control is essential to achieving effective fouling mitigation while preserving energy efficiency and ensuring long term operational reliability in thermofluidic systems. Furthermore, these findings also underscore the need for proactive maintenance and condition-based monitoring to prevent filter saturation and sustain long-term hydraulic efficiency.

The findings of this study reinforce and extend current industry guidance on hydronic system management. Consistent with BSRIA BG 50 [24], the observed recovery in performance under filtered conditions confirms and quantifies the value of proactive filtration and maintenance for sustaining performance, while also highlighting limitations due to saturation. Moreover, the system's sensitivity to magnetite accumulation highlights the complementary importance of water chemistry control and oxygen exclusion, as emphasised in VDI 2035 [23]. While these factors were not directly tested, the results indicate that combining mechanical filtration with preventive water treatment would provide the most robust strategy for mitigating corrosion and fouling in closed-loop hydronic systems.

3.6. Limitations and future works

While this study focused on magnetite-induced fouling, degradation in closed-loop hydronic systems can also result from scaling and microbiological activity, which alter both hydraulic and thermal performance. For example, scaling may impede heat transfer but can also form a protective layer that limits oxygen diffusion and slows magnetite formation [66]. Despite such interactions, magnetite fouling remains the most prevalent and damaging corrosion mechanism in ferrous systems, justifying its use as the primary degradation model. Future work should extend this methodology to include mixed-mode fouling and its combined effects on system efficiency.

Beyond pump–filter interactions, corrosion products can accumulate at valve seats and throttling points, impairing control

accuracy and causing hydraulic instability. Integrating modern pressure-independent control valves (PICVs) can improve hydraulic stability and energy performance under variable loads [67], and their integration with mechanical filtration offers a promising complementary approach for enhancing system resilience. Further studies should also assess fouling behaviour across different valve types such as PICV and pump types, including constant-speed and multistage configurations.

Future development should prioritise developing a predictive maintenance framework that enables data-driven, condition-based interventions. This includes integrating real-time water quality sensing, energy monitoring, and infrared thermographic diagnostics with predictive algorithms capable of identifying early indicators of filter saturation, flow blockages, or abnormal energy demand. Such a system could serve as a digital twin for hydronic networks, providing a dynamic virtual platform for diagnostics, scenario simulation, and proactive optimisation.

Finally, to validate scalability and reliability beyond the laboratory, field deployment in operational hydronic systems is essential. Long-term in-situ monitoring of flow, pressure, temperature, and energy consumption will enable comparison with controlled experiments and the establishment of robust performance benchmarks under real operating conditions. Moreover, as this study employed steady-state flow conditions, future work should examine transient load scenarios, since fluctuating flow and pressure profiles can significantly influence fouling deposition, removal, and overall system stability.

4. Conclusions

This study experimentally demonstrated the impact of corrosion-induced fouling on the energy performance of closed-loop hydronic heating systems, quantifying pump power consumption under varying flow rates, pressures, and fouling conditions. Corrosion was simulated using magnetite to replicate long-term system degradation, while the effectiveness of mechanical filtration in mitigating performance losses was systematically assessed. Therefore the following key conclusions can be drawn:

- Fouling and poor water quality were found to increase pump energy demand by up to 180 %, and under low-pressure conditions could lead to complete pump failure. At higher system pressures (1.5 bar), however, the effect was less pronounced, as increased hydraulic force mitigated particulate accumulation. The results highlight the importance of correct pressurisation and system operation.
- Mechanical filtration restored up to 55 % of corrosion-induced energy losses, yet once the filter reached its sediment-holding capacity, saturation reversed these benefits and led to further hydraulic resistance and energy inefficiency. Furthermore, Sediment capture by the filter increased non-linearly with both pressure and flow rate.
- The findings revealed several interlinked corrosion-related failure modes: **(i)** hydraulic failure resulting from flow obstruction and filter saturation, **(ii)** mechanical failure of pumps due to particulate-induced impeller resistance, and **(iii)** thermal inefficiency caused by fouling deposits that impaired heat transfer. To mitigate these failures and extend system service life, a combined strategy of proper operational control, prevention of oxygen ingress through effective system sealing, and regular filter maintenance is essential. The integration of non-intrusive infrared thermography for blockage detection, as demonstrated in this study, provides a valuable diagnostic tool for condition-based maintenance. Collectively, these measures form a proactive framework for sustaining hydraulic stability, enhancing energy efficiency, and improving the long-term resilience of closed-loop hydronic systems.

This research highlights the often-overlooked impact of corrosion related fouling on hydronic heating system efficiency and demonstrates practical mitigation through mechanical filtration and non-intrusive diagnostics using infrared thermography. This output provides a foundation for future strategies that treat hydronic system maintenance not as reactive upkeep, but as a critical component of smart, low-carbon building operations. The study successfully establishes a validated proof of concept of the approach and the interventions in a controlled laboratory setting, paving the way for broader implementation in real world closed looped building systems across buildings.

CRediT authorship contribution statement

Amr Suliman: Writing – original draft, Visualization, Investigation, Formal analysis, Conceptualization. **Mahroo Eftekhari:** Supervision, Funding acquisition. **Vanda Dimitriou:** Writing – review & editing, Supervision, Investigation. **Yasir Ali:** Writing – review & editing, Visualization, Supervision.

Declaration of competing interest

The authors declare that they have no known competing financial interests or personal relationships that could have appeared to influence the work reported in this paper.

Acknowledgement

The authors would like to acknowledge the funding support received from VEXO international and Engineering and Physical Sciences Research Council (EPSRC) for the undertaking of this work.

Data availability

Data will be made available on request.

References

[1] IEA, Global Alliance for Buildings and Construction, International Energy Agency, and the United Nations Environment Programme, 2019 global status report for buildings and construction: Towards a zero-emission, efficient and resilient buildings, and construction sector, 2019.
[2] HM Government, The UK's plans and progress to reach net zero by 2050, 2024. Available at: https://commonslibrary.parliament.uk/research-briefings/cbp-9888/.
[3] HM Government., 2021., Domestic Heat Distribution Systems: Evidence Gathering., Available at: https://assets.publishing.service.gov.uk/media/606c39c38fa8f515b4067b08/beis-dhds-final-report_1_.pdf.
[4] P. Raftery, R. Singla, H. Cheng, G. Paliaga, Insights from hydronic heating systems in 259 commercial buildings, Energ. Buildings 321 (2024) 114543, https://doi.org/10.1016/j.enbuild.2024.114543.
[5] F. Durrani, R. Wesley, V. Srikandarajah, M. Eftekhari, S. Munn, Predicting corrosion rate in chilled HVAC pipe network: coupon vs linear polarisation resistance method, Eng. Fail. Anal. 109 (2020) 104261, https://doi.org/10.1016/j.engfailanal.2019.104261.
[6] P. West, Prevention of corrosion of metals by water in a closed system, Indust. Eng. Chem. 14 (7) (1922) 601–606, https://doi.org/10.1021/ie50151a006.
[7] J.R. Baylis, Treatment of water to prevent Corrosion1, Indust. Eng. Chem. 19 (7) (1927) 777–781, https://doi.org/10.1021/ie50211a009.
[8] J.R. Baylis, Factors other than dissolved oxygen influencing the corrosion of iron pipes, Indust. Eng. Chem. 18 (4) (1926) 370–380, https://doi.org/10.1021/ie50196a012.
[9] J.R. McDermet, The Degasification of Boiler Feedwater, J. Fluids Eng. 44 (1922) 1297–1306, https://doi.org/10.1115/1.4058224.
[10] O. Opel, T. Eggerichs, T. Otte, W.K. Ruck, Corrosion, scaling and biofouling processes in thermal systems and monitoring using redox potential measurements. Eurocorr 2012 - Safer World through Better Corrosion Control, 2012.
[11] Y. Hou, Y. Pu, S. Chen, Z. Guo, S. Hou, W. Wang, Insight into the corrosion susceptibility and failure mechanism of Cu-Ni alloy pipeline welded joints in simulated marine environment, Eng. Fail. Anal. 160 (2024) 108184, https://doi.org/10.1016/j.engfailanal.2024.108184.
[12] Z. Yan, L. Wang, P. Zhang, W. Sun, Failure analysis of erosion-corrosion of the bend pipe at sewage stripping units, Eng. Fail. Anal. 129 (2021) 105675, https://doi.org/10.1016/j.engfailanal.2021.105675.
[13] X. Xu, S. Liu, K. Smith, Y. Cui, Z. Wang, An overview on corrosion of iron and steel components in reclaimed water supply systems and the mechanisms involved, J. Clean. Prod. 276 (2020) 124079, https://doi.org/10.1016/j.jclepro.2020.124079.
[14] X. Song, G. Zhang, Y. Zhou, W. Li, Behaviors and mechanisms of microbially-induced corrosion in metal-based water supply pipelines: a review, Sci. Total Environ. 895 (2023) 165034, https://doi.org/10.1016/j.scitotenv.2023.165034.
[15] H.M. Hussein Farh, M.E.A. Ben Seghier, R. Taiwo, T. Zayed, Analysis and ranking of corrosion causes for water pipelines: a critical review, npj Clean Water 6 (1) (2023) 65, https://doi.org/10.1038/s41545-023-00275-5.
[16] J. Liu, H. Chen, L. Yao, Z. Wei, L. Lou, Y. Shan, S.D. Endalkachew, N. Mallikarjuna, B. Hu, X. Zhou, The spatial distribution of pollutants in pipe-scale of large-diameter pipelines in a drinking water distribution system, J. Hazard. Mater. 317 (2016) 27–35, https://doi.org/10.1016/j.jhazmat.2016.05.048.
[17] S. Zhang, Y. Tian, H. Guo, R. Liu, N. He, Z. Li, W. Zhao, Study on the occurrence of typical heavy metals in drinking water and corrosion scales in a large community in northern China, Chemosphere 290 (2022) 133145, https://doi.org/10.1016/j.chemosphere.2021.133145.
[18] M. Swift, Corrosion under Insulation on Industrial piping - a Holistic Approach to Insulation System Design, in: CORROSION 2019. Nashville, TN., AMPP, 2019, pp. 1–15, https://doi.org/10.5006/C2019-13042.
[19] T.P. Hoar, Review Lecture-Corrosion of metals: its cost and control, Proc. Royal Soc. London. A. Math. Phys. Sci. 348 (1652) (1976) 1–18.
[20] O. Opel, M. Wiegand, K. Neumann, M. Zargari, S. Plesser, Corrosion in heating and cooling water circuits - a field study, Energy Procedia 155 (2018) 359–366, https://doi.org/10.1016/j.egypro.2018.11.042.
[21] A. Suliman, M. Eftekhari, V. Dimitriou, D. Tseno, Water quality in HVAC hydronic systems: an international review, ASHRAE Trans. 130 (1) (2024) 982–990, https://doi.org/10.63044/w24sul117.
[22] C. Parsloe, M. Ronceray, Pre-commissioning cleaning of Pipework Systems, 6th edition, Building Services Research and Information Association (BSRIA), Bracknell, 2021.
[23] Verein Deutscher Ingenieure, Prevention of damage in water heating installations Water-side corrosion VDI 2035 Blatt 2 / Part 2 VDI-Gesellschaft Bauen und Gebäudetechnik VDI-Handbuch Technische Gebäudeausrüstung, Band 3: Sanitärtechnik VDI-Handbuch Technische Gebäudeausrüstung, Band 4: Wärme-/Heiztechnik, 2009. www.vdi.de/2035.
[24] P. Simpson, Water treatment for closed heating and cooling systems, 2nd ed.,, Building Services Research and Information Association (BSRIA), Bracknell, 2021.
[25] D. Johnston, D. Glew, D. Miles-Shenton, M. Benjaber, R. Fitton, Quantifying the performance of a passive deaerator in a gas-fired closed loop domestic wet central heating system, Build. Serv. Eng. Res. Technol. 38 (3) (2017) 269–286, https://doi.org/10.1177/0143624416675391.
[26] E. Jansen, R. Vandenbulcke, W. Denckens, G. Helms, H. Elkhaoui, J. VandePaer, Comparative Research Flamco, The Department of Industrial Science and Technology, Karel de Grote University College, Antwerp, Belgium, 2011.
[27] A. Suliman, D. Wilkinson, V. Dimitriou, M. Eftekhari, D. Tseno, A visualization of the impact of water quality in the energy performance of closed looped heating systems using IR Thermography, ASHRAE Trans. 129 (2) (2023).
[28] B. Kuźnicka, Erosion–corrosion of heat exchanger tubes, Eng. Fail. Anal. 16 (7) (2009) 2382–2387, https://doi.org/10.1016/j.engfailanal.2009.03.026.
[29] A. Adamkowski, A. Henke, M. Lewandowski, Resonance of torsional vibrations of centrifugal pump shafts due to cavitation erosion of pump impellers, Eng. Fail. Anal. 70 (2016) 56–72, https://doi.org/10.1016/j.engfailanal.2016.07.011.
[30] U. Klein, A. Zunkel, A. Eberle, Breakdown of heat exchangers due to erosion corrosion and fretting caused by inappropriate operating conditions, Eng. Fail. Anal. 43 (2014) 271–280, https://doi.org/10.1016/j.engfailanal.2014.03.019.
[31] H.S. Kim, J. Kim, S. Sohn, J. Seo, Y. Cho, H.J. Park, Experimental and numerical investigation on the fouling of a river water source heat pump system, Appl. Therm. Eng. 245 (2024) 122784, https://doi.org/10.1016/j.applthermaleng.2024.122784.
[32] Y.R. Yoo, D.H. Kim, G.B. Kim, S.Y. Won, S.H. Choi, Y.S. Kim, Galvanic corrosion between component parts of aluminum alloys for heat exchanger of automobile, Corrosion Sci. Technol. 22 (5) (2023) 322–329.
[33] O. Opel, T. Eggerichs, T. Otte, W.K. Ruck, Monitoring of microbially mediated corrosion and scaling processes using redox potential measurements, Bioelectrochemistry 97 (2014) 137–144, https://doi.org/10.1016/j.bioelechem.2013.11.004.
[34] J. Starosvetsky, D. Starosvetsky, R. Armon, Identification of microbiologically influenced corrosion (MIC) in industrial equipment failures, Eng. Fail. Anal. 14 (8) (2007) 1500–1511, https://doi.org/10.1016/j.engfailanal.2007.01.020.
[35] J. Jiang, F. Zhu, K. Li, J. Du, Y. Liu, X. Liu, S. Yu, Calcium sulfate scale control technology for circulating cooling water systems: a review, J. Ind. Eng. Chem. (2025), https://doi.org/10.1016/j.jiec.2025.05.029.
[36] Z. Qiankun, S. Yafei, R. Sixian, L. Huifeng, Z. Xingjiang, Corrosion failure analysis on heat exchanger pipes, J. Fail. Anal. Prev. 17 (2) (2017) 349–353, https://doi.org/10.1007/s11668-017-0248-9.
[37] B. Raman, D.M. Hall, S.J. Shulder, M.F. Caravaggio, S.N. Lvov, An experimental study of deposition of suspended magnetite in high temperature-high pressure boiler type environments, Colloids Surf A Physicochem Eng Asp 508 (2016) 48–56, https://doi.org/10.1016/j.colsurfa.2016.08.018.
[38] H.H. Hosamo, P.R. Svennevig, K. Svidt, D. Han, H.K. Nielsen, A Digital Twin predictive maintenance framework of air handling units based on automatic fault detection and diagnostics, Energ. Buildings 261 (2022) 111988, https://doi.org/10.1016/j.enbuild.2022.111988.

[39] X. Xie, J. Merino, N. Moretti, P. Pauwels, J.Y. Chang, A. Parlikad, Digital twin enabled fault detection and diagnosis process for building HVAC systems, Autom. Constr. 146 (2023) 104695, https://doi.org/10.1016/j.autcon.2022.104695.
[40] S. Munn, Testing the water – tackling corrosion in pipework, CIBSE Journal, [Online]. 2016. Available at: https://www.cibsejournal.com/technical/testing-the-water-tackling-corrosion-in-pipework/.
[41] M.P. Weberski Jr, B. Chen, April. Next Generation Closed Loop Corrosion Inhibitors: increasing Reliability & Decreasing Environmental Impact. NACE Corrosion, NACE, 2021.
[42] J.N. Patel, A. Chang, H. Shahbazbegian, B. Kaminska, Adaptive corrosion protection system using continuous corrosion measurement, parameter extraction, and corrective loop, Int. J. Corrosion 2016 (1) (2016) 9679134, https://doi.org/10.1155/2016/9679134.
[43] J. Lane, Y. Cho, W. Kim, Pulsed-power water treatment as a green scale inhibitor for HVAC and once-through industrial systems. NACE Corrosion, NACE, 2004.
[44] B.P. Boffardi, Water treatment for HVAC & R systems, ASHRAE J. 41 (5) (1999) 52–56.
[45] K. Alfredo, E. Bedard, H.Y. Buse, M. Cazals, P. Francisco, J. Lee, S. Masters, E. Osann, A. Stillwell, P. Westerhoff, T.A. Bartrand, Ten questions concerning water quality in building hot water systems, Build. Environ. 275 (2025) 112803, https://doi.org/10.1016/j.buildenv.2025.112803.
[46] I. Skoczko, E. Szatyłowicz, Treatment method assessment of the impact on the corrosivity and aggressiveness for the boiler feed water, Water 11 (10) (2019) 1965, https://doi.org/10.3390/w11101965.
[47] E.J. Daamen, J.W. Wouters, J.T.G. Savelkoul, Side stream biofiltration for improved biofouling control in cooling water systems, Water Sci. Technol. 41 (4–5) (2000) 445–451, https://doi.org/10.2166/wst.2000.0478.
[48] L. Li, Y.T. Ge, X. Luo, S.A. Tassou, Experimental investigations into power generation with low grade waste heat and R245fa Organic Rankine Cycles (ORCs), Appl. Therm. Eng. 115 (2017) 815–824, https://doi.org/10.1016/j.applthermaleng.2017.01.024.
[49] M. Dongellini, C. Naldi, S. Cancellara, G.L. Morini, Experimental measurements of thermal–hydraulic performance of aluminium-foam water-to-air heat exchangers for a HVAC application, Appl. Therm. Eng. 213 (2022) 118716, https://doi.org/10.1016/j.applthermaleng.2022.118716.
[50] X.Y. Zhang, Y.T. Ge, P.Y. Lang, Experimental investigation and CFD modelling analysis of finned-tube PCM heat exchanger for space heating, Appl. Therm. Eng. 244 (2024) 122731, https://doi.org/10.1016/j.applthermaleng.2024.122731.
[51] A. Suliman, D. Wilkinson, M. Eftekhari, V. Dimitriou, Investigating the efficiency of mechanical filtration in restoring the efficiency of a corroded closed-looped heating and cooling system. CIBSE Technical Symposium, Glasgow, 2023 https://hdl.handle.net/2134/22673368.v1.
[52] Health and Safety Executive, Managing legionella in hot and cold-water systems, 2024. Available at: <https://www.hse.gov.uk/legionnaires/hot-and-cold.htm>.
[53] CIBSE, CIBSE Guide B1: Heating, Vol. 30, London: The Chartered Institution of Building Services Engineers, 2016. Available at: www.cibse.org, IBN: 9781906846732.
[54] ASHRAE, ASHRAE handbook; HVAC Systems and Equipment. American Society for Heating, Refrigeration and Air -Conditioning Engineering, ASHRAE, Atlanta, GA, 2015.
[55] British Standards Institute, BS 6700 Design, installation, testing and maintenance of services supplying water for domestic use within buildings and their curtilages Specification, British Standard Institute, 2009. Available at: https://www.bsigroup.com/en-GB/.
[56] K. De Cuyper, K. Dinne, TVN 278: Hot Water heating systems: recommendations to prevent deposits and corrosion, The Scientific and Technical Centre for the Construction Industry WTCB, 2021. Available at: https://www.buildwise.be/en/publications/technical-information/278/.
[57] Ideal Heating, How long does a boiler last?, n.d. [online] Available at: https://idealheating.com/tips-and-advice/how-long-does-a-boiler-last.
[58] K.K. McKee, G. Forbes, I. Mazhar, R. Entwistle, I. Howard, A review of major centrifugal pump failure modes with application to the water supply and sewerage industries. ICOMS Asset Management Conference, QLD, Australia, Gold Coast, 2011.
[59] S. Bandi, J. Banka, A. Kumar, A.K. Rai, Effects of sediment properties on abrasive erosion of a centrifugal pump, Chemical Engineering Science 277 (2023) 118873, https://doi.org/10.1016/j.ces.2023.118873.
[60] M.M.M. Awad, S.M. Abd El-Samad, R.E. Gad, E.L. Asfour, Effect of flow velocity on the surface fouling, MEJ-Mansoura Engineering Journal 32 (1) (2020) 27–37.
[61] J. Song, Z. Liu, Z. Ma, J. Zhang, Experimental investigation of convective heat transfer from sewage in heat exchange pipes and the construction of a fouling resistance-based mathematical model, Energy and Buildings 150 (2017) 412–420, https://doi.org/10.1016/j.enbuild.2017.06.025.
[62] Department for Energy Security and Net Zero, Greenhouse gas reporting: conversion factors 2025, 2025. GOV.UK. [online] Available at: https://www.gov.uk/government/publications/greenhouse-gas-reporting-conversion-factors-2025.
[63] L. Yang, H. Fu, H. Liang, Y. Wang, G. Han, K. Ling, Detection of pipeline blockage using lab experiment and computational fluid dynamic simulation, J. Petrol. Sci. Eng. 183 (2019) 106421, https://doi.org/10.1016/j.petrol.2019.106421.
[64] F. García-Ávila, C. Zhindón-Arévalo, R. Álvarez-Ochoa, S. Donoso-Moscoso, M.D. Tonon-Ordoñez, L.F. del Pino, Optimization of water use in a rapid filtration system: a case study, Water-Energy Nexus 3 (2020) 1–10, https://doi.org/10.1016/j.wen.2020.03.005.
[65] H.S. Kandra, A. Deletic, D. McCarthy, Assessment of impact of filter design variables on clogging in stormwater filters, Water Resources Manag. 28 (7) (2014) 1873–1885, https://doi.org/10.1007/s11269-014-0573-7.
[66] A. Shokri, M.S. Fard, Principles, operational challenges, and perspectives in boiler feedwater treatment process, Environ. Adv. 13 (2023) 100389, https://doi.org/10.1016/j.envadv.2023.100389.
[67] C. Naldi, M. Dongellini, G.L. Morini, E.R. di Schio, The adoption of pressure independent control valves (PICVs) for the simultaneous optimization of energy consumption and comfort in buildings, Energ. Build. 287 (2023) 112969.